PCCP

Accepted Manuscript

ROYAL SOCIETY OF CHEMISTRY

www.rsc.org/pccp

Journal Name

ARTICLE TYPE

Cite this: DOI: 10.1039/xxxxxxxxxx

Role of electrostatic interactions on the adsorption kinetics of nanoparticles at fluid-fluid interfaces†

Venkateshwar Rao Dugyala,[a] Jyothi Sri Muthukuru,[a] Ethayaraja Mani,*[a] Madivala G Basavaraj*[a]

Received Date
Accepted Date

DOI: 10.1039/xxxxxxxxxx

www.rsc.org/journalname

The adsorption of particles to the fluid-fluid interface is a key factor for the stabilization of fluid-fluid interfaces such as those found in emulsions, foams and bijels. However, for the formation of stable particle-laden interfaces, the particles must migrate to the interface from the bulk. Recent studies show that the adsorption of particles to the interface formed during emulsification is influenced by the surface charge of the particles. To further investigate this phenomena, we study the effect of surface charge of particle on the adsorption kinetics of particles to the oil-water interface. By suspending a drop of aqueous dispersion of charge stabilized nano particles in decane, the adsorption dynamics of particles to the decane-water interface is studied using the dynamic surface tension measurements. When the particles are highly charged (low salt), a negligible change in the interface tension is observed indicating that almost no particles are adsorbed. These results show that the charged particles experience an energy barrier when they approach the interface. But when the particles surface charge is screened by the addition of monovalent salt, a significant reduction in surface tension is observed indicating the migration and adsorption of particles to the decane-water interface. We estimate the effective diffusivity of particles to the interface by analyzing the initial decay in the measured surface tension by considering particle laden drops containing different amount of salt using the modified Ward and Tordai theory. This effective diffusivity is used to calculate the energy barrier for the adsorption of particles to the interface. The energy barrier from the analysis of dynamic surface tension data agrees well with the concept of image charge repulsion which inhibits the adsorption of highly charged particles to the interface. By considering various types of relevant interactions, we derive an analytical expression that qualitatively captures the effect of surface charge on the equilibrium surface coverage of particles at the drop surface.

1 Introduction

The spontaneous or forced adsorption of particles to the liquid-liquid or liquid - air interface is one amongst many strategies to create different functional materials using, for example, Pickering emulsion [1–5], foam [6–9] and bijel [10–12] structures as templates. These functional materials have diverse applications in different fields such as oil recovery, drug delivery, catalysis and membrane technology. The crucial part in the design of these novel functional materials is the migration and irreversible adsorption of particles at the interface leading to the stabilization of incompatible interfaces. To create stable particle laden interfaces, it is a general practice to add certain additives such as surfactants or electrolytes. While the addition of salt is known to effect Pickering emulsion stabilization, the role of electrostatic interactions and the mechanism that leads to the formation of stable particle-laden interface with the addition of salt is poorly understood.

In general, to form Pickering emulsions external energy is used to create new interface either via manual or mechanical mixing. This applied energy will facilitate the migration of the particles from the bulk to the newly created interface. It has been shown recently that in order to form stable particle stabilized emulsions, the magnitude of external energy required is higher if the particles are highly charged.[5] This has been attributed to the image charge induced energy barrier that must be overcome when the particles approach near to the interface. The estimation of this energy barrier is important because it also affects the adsorption kinetics of particles to the interface.[13,14] In this article, we provide a simple methodology for the estimation of this energy bar-

[a] Polymer Engineering and Colloid Science Lab (PECS Lab), Department of Chemical Engineering, Indian Institute of Technology Madras, India; E-mail: basa@iitm.ac.in;ethaya@iitm.ac.in

† Electronic Supplementary Information (ESI) available: [early time plots for different salt concentration]. See DOI: 10.1039/b000000x/

rier through dynamic surface tension measurements.

Planar particle monolayers or two-dimensional particle laden flat interfaces are widely studied in literature. For example, ordering of particles in the monolayer, structural transitions, aggregation kinetics and influence of particle shape on the structural arrangement have been widely investigated.[15–19] It must be noted that in these studies, particles in a suitable medium are spread typically using a micro-syringe such that particles invariably accumulate at the interface. This enables the study of various phase transitions and structure-property correlation in particle monolayer at flat interfaces. Comparatively, however, a few authors have studied the adsorption kinetics of particles to the fluid-fluid interfaces.[20–27] In most of the studies, the authors investigated the adsorption kinetics by using the pendent drop technique, which is a widely used method to investigate the adsorption kinetics of surfactants to interfaces. Nanoparticles with different stabilizers (tri-n-octylphosphine oxide (TOPO)-stabilized CdSe nanoparticles or alkaline caped gold nanoparticle or protein coated nanoparticles) have been used to study the effect of particle concentration and size on the adsorption kinetics.[22,23,28,29] From these experiments, the authors observed an increase in the adsorption rate with increase in particle concentration. Recently, Nelson *et al.* investigated the adsorption of iron oxide-poly (ethylene glycol) core shell particle to the water-decane interface.[26] The particle adsorption rate is observed to be proportional to the bulk concentration and at the maximum coverage the particle-laden interface still behaved as a fluid. The use of pendant drop technique for dynamic and equilibrium surface tension measurements showed significant higher interfacial activity of Janus nanoparticles of controlled amphiphilicity.[25] Deshmukh *et al.* studied the effect of particle surface chemistry on adsorption dynamics by using Pendant drop method. The interfacial tension reduction is higher with modified gold nanoparticles by using dodecanethiol (DDT) or octadecanethiol (ODT) when compared to the bare gold particles. The difference has been attributed to the hydrophobic nature of the grafted gold nanoparticles. More recently, adsorption of soft microgel particles has been investigated.[21] While diffusion of the particles from bulk to the interface controls the adsorption of these particles at short times, at long times, the crowding of particles at the interface creates an entropic barrier for the new particles to adsorb to the interface.

Though the adsorption of particle to the interface is thermodynamically favored, their adsorption kinetics depends on a number of parameters. Typically, the adsorption kinetics of nanoparticles measured via the pendant drop method is analyzed to understand the effect of various parameters on adsorption kinetics. The early and late stage adsorption process monitored via these dynamic surface or interfacial tension (DST) experiments is generally modeled using the Ward and Tordai (1946) theory.[30] According to this theory the kinetic process depends on the particle size and concentration - that is adsorption is purely diffusion controlled. In the absence of any external energy barrier, the time required for a particle to reach the interface from the bulk depends only on the particle diffusivity because this theory assumed instantaneous adsorption to the interface. However, in the presence of an energy barrier, the rate of adsorption of particles to the interface decreases and therefore both diffusion and energy barrier become important. Several theories were put forward to include diffusion and adsorption kinetics in the overall kinetics of adsorption, especially for surfactant adsorption studies.[31–34]

Recently, Bizmark *et al.*, studied the kinetics of adsorption of ethyl cellulose nanoparticles at water-air interface.[20] The asymptotic solutions of Ward and Tordai theory in the limit of $t \to 0$ and $t \to \infty$ are used to explain experimentally observed reduction of surface tension with time. In particular, for $t \to 0$, in other words the initial decay of surface tension is given by

$$\gamma = \gamma_0 - 2N_A C_0 \Delta E \sqrt{\frac{Dt}{\pi}} \quad (1)$$

In this equation, γ is interfacial tension at any given time t , γ_0 is the pure water-oil interfacial tension, N_A is the Avogadro number, C_0 is the initial bulk concentration of particles and ΔE is the detachment energy of the particle. The above equation assumes that the adsorption of particles to the interface is instantaneous. Bizmark *et al.* used eqn1 to fit the initial γ vs $\sqrt{t}$ data with ΔE as the fitting parameter for several initial concentration of particles C_0. While the authors observe that ΔE depends on particle concentration. However, by definition, ΔE is defined as

$$\Delta E = \pi r^2 \gamma_0 (1 - |\cos\theta|)^2 \quad (2)$$

with r as the radius of the particles, γ_0 is the pure oil-water interfacial tension and θ as the three phase contact angle of particle at the interface. In their study, adsorption of particles to the interface is dominated by the hydrophobic attraction between the particle and the interface than the electrostatic repulsions between the particle and the interface. However, when the particles are highly charged, the contribution to repulsive interactions due to electrostatic interaction between the particle and the interface, the particle and image charge, and repulsion between approaching particle and particles already adsorbed at the interface are to be considered. Previous studies have not considered these effect in understanding adsorption of nanoparticles examined via dynamic surface tension measurements.

In this work we investigate the effect of particle surface charge on the adsorption kinetics. From the study of dynamic surface tension of aqueous drops containing charge stabilized particles suspended in an oil medium, we demonstrate the role of particle electrostatic interactions on their adsorption to water-oil interface. Aqueous suspensions containing mono-disperse silica particles of known surface charge are used in all the experiments. When the particles are highly charged, the change in the surface tension with time is negligible. However, as the surface charge on the particle is screened by the addition of a monovalent salt, a decrease in surface tension is observed. This reduction in surface tension is attributed to the adsorption of particles to the oil-water interface. By analyzing the initial reduction in the interfacial tension measured as a function of salt concentration using the eqn 3, we calculate the effective diffusivity of particles to the interface by assuming ΔE is constant. The effective diffusivity is found to be a few orders of magnitude less than Stoke-Einstein's diffusivity indicating the existence of an energy barrier for the adsorption

of particles to the decane-water interface. The energy barrier is found to decrease with increase in salt concentration. The energy barrier from the analysis of DST data is compared with the calculation of the overall interactions in the vicinity of the interface. The energy barrier obtained from the analysis of DST measurements agree well with overall interaction energy barrier calculations when the concept of image charge repulsion is incorporated. The effect of particle concentration on the adsorption kinetics is also studied. An analytical expression that captures the effect of surface charge on the equilibrium surface coverage of particles at the drop surface is derived. The predictions of the analytical equation is in qualitative agreement with experimentally observed dynamic surface tension measurements.

2 Methods

Charge stabilized mono-disperse silica nanoparticle suspension (Ludox SM30) was obtained from the Sigma Aldrich. This suspension contains negatively charged particles at a concentration of 30 % by weight. The silica suspension was used as received. The hydrodynamic diameter of these particles as measured by dynamic light scattering technique was 10.3 ± 3.2 nm. For adsorption studies, decane (Merck, India) was used as oil medium. The decane was treated with activated alumina to remove water soluble impurities if any. A series of silica nanoparticle suspensions of concentration ranging from 0.25 to 1 wt% were prepared from the stock suspensions by dilution with the deionized water from MilliQ (18.2 MΩ.cm). In order to screen the surface charge of particles, monovalent sodium chloride (NaCl) salt was used. The electrophoretic mobility of particle was measured with electrophoretic dynamic light scattering (Nanopartica, Horiba, Japan). From the mobility data the particle zeta potential was calculated by using the Smoluchowski equation.[35]

The pendant drop method was used to measure the interfacial tension as a function of time. The dynamic interfacial tension of silica particle suspension-decane was measured with the Goniometer (GBX, Digidrop, France). All experiments were conducted at a constant temperature of $28 \pm 2^{\circ}C$. Two types of experiments were performed. In first set of experiments, the NaCl concentration was varied (from 0.001M to 0.1M), but the concentration of particles in the suspension was kept constant at 1 wt %. In the second set of experiments, the concentration of particles in the suspension were systematically increased from 0.25 to 1 wt % at a fixed NaCl concentration. The schematic of the experimental setup is shown in Fig. 1. A transparent rectangular disposable plastic cuvette (poly ethylene) was filled with decane. An aqueous drop containing the charged silica particles at known salt concentration was suspended in the decane medium with the help of a syringe. A 20 μl suspension droplet was used in all the experiments. A series of time sequence images of the drop were captured for 2500 sec at frame rate of 30 images per minute. The captured images were used to calculate the interfacial tension by the drop shape analysis wherein the contour of drop was fitted with the Young Laplace equation to determine the interfacial tension. All the experiments were repeated at least 3 times for consistency.

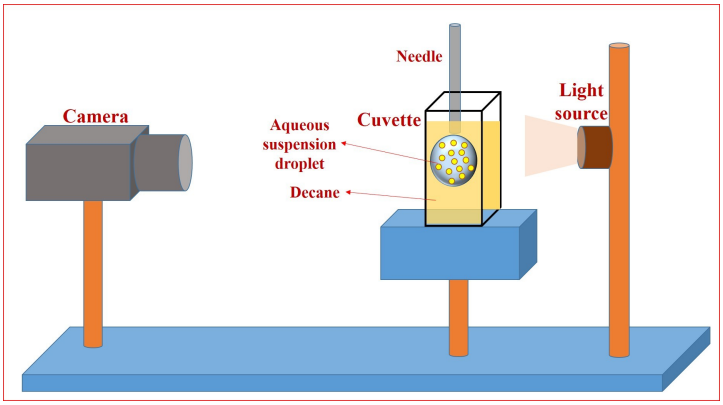

Fig. 1 The schematic of experimental setup for dynamic surface tension (DST) measurements using the pendant drop method. A Ludox SM30 silica nanoparticle suspension drop suspended in a continuous decane medium is imaged with the help of a CCD camera.

3 Results and discussion

3.1 Effect of addition of salt on the adsorption kinetics

In all the experiments the concentration of particles in the aqueous suspension drop is fixed at 1 wt%. The surface charge on the particle is screened by the addition of appropriate quantity of sodium chloride (NaCl). The concentration of NaCl in the drop is varied from 0.001 M to 0.1 M. This helps us study the sole influence of particle charge effect on the adsorption dynamics as all other conditions are identical. Initially, control experiments are carried out with pristine water drop without any particles and water drop containing 1 wt% particles without any salt. The dynamic surface tension data recorded are shown in Fig. 2. In the control experiment without particles and salt i.e., for the decane-water interface the interfacial tension is almost constant. A negligible change in the interfacial tension is observed which may be due to the presence of small amount of water soluble impurities that are probably not removed during the treatment of decane with activated alumina. Similarly, with 1 wt% suspension drop without any NaCl - that is - when the drop contains highly charged particles, there is almost no change in the interfacial tension. However, as the concentration of NaCl in the suspension is systematically increased, the dynamic interfacial tension data showed a sharp decrease as shown in Fig. 2. From Fig.2, a significant change in the interface surface tension is observed with time when the salt concentration is high (0.1M).

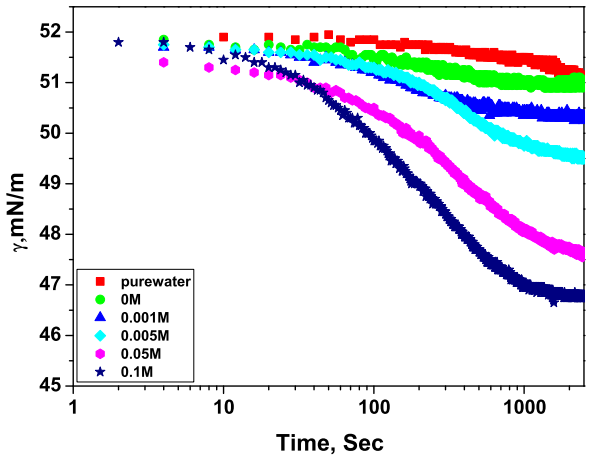

Fig. 2 The dynamic surface tension of decane-aqueous silica nanoparticle suspension as a function of NaCl concentration. The particle concentration is 1wt% in all the experiments. A significant decrease in interfacial tension can be seen as the salt concentration is increased.

This decrease is significant at initial time and thereafter, the interfacial tension change is very sluggish reaching a plateau at later times. In case of lowest salt condition used (0.001M), the change in the interfacial tension is very similar to the case of salt free suspension. A closer look at Fig 2 clearly indicates that in the case of high salt concentration, the surface tension data show different slopes i.e., the adsorption rate of particles to the interface at different times. As the particle coverage increases, the adsorbed particles create additional energy barrier for the particles to reach the interface from the bulk. This resistance is a result of the electrostatic interaction between the adsorbed particles (dipole-dipole interaction), interaction between the particle near the interface and adsorbed particle (electrostatic double layer interaction), probability to find a particle free interface, which is a function of particle coverage and rearrangement of the particles at interface.[20,28,36] Since these resistances start to dominate at later times, the change in the surface tension is sluggish. The above resistance are negligible when the particle coverage is less since the water-decane interface is free of particles. At initial times, the change in the surface coverage is significant (higher slope) and the initial decay depends on the salt concentration. A significant change in the initial slope for different salt concentration clearly indicates an energy barrier for particle adsorption at the interface. In the following section we estimated the energy barrier by analyzing the early time DST data where other energy barriers due to already adsorbed particles are not significant.

3.2 Modeling of nanoparticle adsorption

In the pendant drop experiments, unlike emulsification process, no mechanical energy is provided externally to promote particle adsorption to the interface. That is the particles approach the interface solely by diffusion. Generally, the adsorption of particles at interface is either diffusion controlled or energy barrier controlled or a combination of both. In case of diffusion controlled process, the transfer of particles from the bulk to the interface is controlled by the particles diffusivity and the energy barrier for the particle adsorption at the interface is neglected. However, Liggieri *et al.*[33] and Ravera *et al.*[32] proposed an effective diffusion model, where the energy barrier for the particle adsorption at the interface is included. The effective diffusivity model has previously been used for the protein adsorption at interface and diffusion of charged particle in porous materials.[37–39]

At initial times ($t \to 0$), the adsorption is limited by the diffusion process as the interface is free of particles. Once nanoparticle adsorb to the interface it is very unlikely that it detaches from the interface due to high detachment energy ($\sim 50 k_B T$). Therefore, we use modified diffusion controlled (Ward and Tordai) theory to model the early time adsorption process. We can infer from the experimental results in Fig. 2 that with the addition of salt, there is adsorption of particles to the interface which is associated with the change in interfacial tension. Thus, it clearly indicates the presence of an energy barrier as the particles approach near to the interface. This energy barrier of (all kinds such as particle-interface interactions and image charge repulsion) will influence the particles flux to the interface. To include the energy barrier effects on adsorption process, we replace the particle diffusivity D with the effective diffusion coefficient D_{eff} in the eqn 1. We therefore calculate the effective diffusivity of the particles by modeling the early time dynamic surface tension data using the adsorption kinetic model (eqn 3)[20]

$$\gamma = \gamma_0 - 2N_A C_0 \Delta E \sqrt{\frac{D_{eff} t}{\pi}} \tag{3}$$

Where, D_{eff} is the effective diffusion constant. The particle detachment energy from the interface was calculated from eqn 2. Since the actual position of nanoparticles with respect to the interface was difficult to measure, the contact angle of micron sized silica particles that has been reported was used ($\theta = 38$).[40,41] The eqn 3 can be expressed as a linear equation

$$\gamma = P1 - P2\sqrt{t} \tag{4}$$

Where, $P1$ is the pure water-oil surface tension (γ_0) and $P2$ is $2N_A C_0 \Delta E \sqrt{\frac{D_{eff}}{\pi}}$. For further analysis, the early time DST data from 0 to 100 s was used. A typical plot showing the early time DST data fitted with eqn 4 for a drop containing 1 wt% particle concentration and 0.1M salt concentration is shown in Fig 3. By using the fitting parameters the effective diffusivity of the particles (D_{eff}) was calculated to be 2.40×10^{-14} m^2/s, which is about three order of magnitude lower than Stokes-Einstein particle diffusivity of 4.98×10^{-11} m^2/s. The Stokes-Einstein equation[35] ($D_0 = k_B T / 6\pi\mu r$) is used to calculate particle bare diffusivity, where k_B is the Boltzmann constant, T is aqueous suspension temperature ($T = 28°C$), r is the particle radius ($r = 5nm$) and μ is solvent (water) viscosity ($\mu = 0.83cP$). As the concentration of salt in the suspension is increased, the effective diffusivity is found to increase. Table 1 shows the effective diffusivity data calculated at the NaCl concentrations studied. From Table 1, the parameter P1 is $\cong$ 52 mN/m and P2 is found to increase with salt

Table 1 The fitted parameter for the suspension contains 1 wt% particles with different salt concentration. The effective diffusion and energy barrier is calculated from the model. The actual diffusion of the particle is 4.98 $\times 10^{-11} m^2/s$

Salt concentration (M)	Fitting parameter P1 (mN/m)	Fitting parameter P2 ($mN/mt^{0.5}$)	D_{eff} m^2/s (10^{-15})	U/k_BT (from eq(5))
0.001	51.96±0.01	0.0630±0.0026	1.73±0.14	10.27±0.07
0.005	51.89±0.11	0.0725±0.0017	2.29±0.11	9.98±0.05
0.05	51.95±0.20	0.1305±0.0004	7.41±0.05	8.81±0.01
0.1	52.35±0.04	0.2381±0.0040	24.8±0.08	7.61±0.04

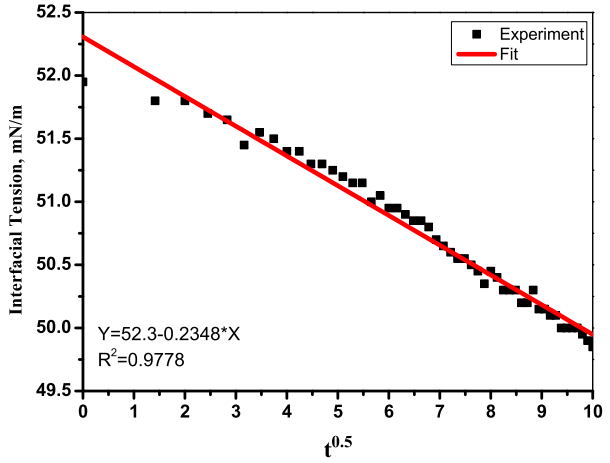

Fig. 3 Plot of early time surface tension Vs $\sqrt{t}$ data (from 0 to 100 sec) for suspension containing 1 wt% particles and 0.1M NaCl concentration. The solid line represents fit that assumed to be adsorption kinetics model eqn 4. The fitting parameters and R^2 values are shown in the inset of the plot.

concentration.

We attribute the change in the effective diffusivity to the energy barrier for adsorption of particles at the interface. The effective diffusivity D_{eff} due to the presence of an energy barrier U is related to the bare diffusion coefficient D_0 (without any adsorption barrier) by[32,33]

$$D_{eff} = D_0 \exp\left(-\frac{U}{k_B T}\right) \quad (5)$$

The bare diffusivity of the particle D_0 is calculated by using the Stokes-Einstein equation. By using the eqn 5, the energy barrier (U) was calculated from the effective diffusivity values. The energy barrier at 0.1 M salt concentration was 7.61 k_BT. The effective diffusivity and energy barrier at different salt concentration tabulated in Table 1, clearly indicate the reduction in energy barrier with increase in salt concentration. At low salt concentration, the thermal energy of the particles is not enough to overcome the energy barrier. Since the particles used are electrostatically stabilized, the energy barrier is likely to be of electrostatic origin and therefore we calculate the DLVO interactions near the interface.

3.3 Calculation of interaction of charged particle close to the interface

The energy barrier obtained from modeling the time variation of interfacial tension is compared with the possible charge induced energy barrier for particle adsorption to decane-water interface. We calculated the overall interactions in the vicinity of the interface. It is known that under experimental conditions, the interface is negatively charged.[42] The overall DLVO interactions near the interface is summation of 1) the van der Waals interaction between the particles and charged interface 2) the electric double layer interaction due to surface charge of the interface and the particles. Under experimental conditions, both the particles and the interface are always negatively charged (see Table 2), therefore, it can be argued that the repulsive barrier is due to particle-interface repulsion.

Table 2 The zeta potential of negatively charged Ludox silica nanoparticles as a function of salt concentration. The interface zeta potential is obtained by the extrapolation of data from the literature.[42]

Salt concentration M	Particle zeta potential (mV)	Interface zeta potential (mV)[42]
0	-63.6±1.24	
0.001	-48.9±1.31	-60
0.005	-40±1.51	-45
0.05	-24.5±4.91	-30
0.1	-15±3.55	-20

However, it was recently shown that a repulsive barrier still exists when the particles and interface are oppositely charged - that is when particles are positively charged and interface is negatively charged. This repulsive barrier was attributed to the image charge effects.[5] In the overall calculations, we therefore included that $U_{total} = U_{vdw} + UE_{p-int} + UE_{p-image}$. Where, U_{vdw} is van der Waals interaction between the particle and the interface, UE_{p-int} is electrostatic interaction between the particle and the interface, and $UE_{p-image}$ is the particle-image charge interaction.

The nature of the interaction between the particle and the interface can be considered as interaction between a spherical particle and a flat plate. The van der Waal interaction between the particle and interface is calculated by using the eqn 6.[43]

$$U_{vdw} = -\frac{A}{6}\left[\frac{r}{h} + \frac{r}{h+2r} + \ln\left(\frac{h}{h+2r}\right)\right] \quad (6)$$

Where, A is the effective Hamaker constant, r is the particle radius and h is the surface to surface distance between the particle

and interface. While calculating the van der Waals interaction between the particle and the interface, we assume that the spherical particles are interacting with a slab of decane through water medium. The effective Hamaker constant is calculated from the mixing rule as $A \approx \sqrt{A_{oil} - A_{water}}\sqrt{A_{particle} - A_{water}}$ where, A_{oil} is the Hamaker constant for the decane $(5 \times 10^{-20} J)$, A_{water} is the Hamaker constant for water $(4 \times 10^{-20} J)$ and $A_{particle}$ is Hamaker constant of silica particles $(6.5 \times 10^{-20} J)$.[35,44] The effective Hamaker constant was calculated to be $\approx 1.3 \times 10^{-21} J$.

In the case of liquid drop containing charged particles suspended in another fluid, the origin of image charge effect is due to the difference in the dielectric constants of the fluids across the interface. The image charge is calculated by using the eqn 7.[5]

$$q_{image} = q_{particle}\frac{\varepsilon_1 - \varepsilon_2}{\varepsilon_1 + \varepsilon_2} \tag{7}$$

In eqn 7, ε_1 is the dielectric constant of the medium which contains the charged particle and ε_2 is the dielectric constant of the particle free medium. From the eqn 7, when a charged particle present in a high dielectric medium such as water ($\varepsilon_1 \approx 78$) approaches an interface across which a low dielectric medium is present (decane $\varepsilon_2 \approx 2$) , the particles experience a repulsion due to a like-charged particle present across the interface (See Fig. 4). The image charge surface potential is calculated by using Grahame equation.[45]

$$\Psi_{image} = \frac{2k_BT}{e}\sinh^{-1}\left(\frac{\varepsilon_1 - \varepsilon_2}{\varepsilon_1 + \varepsilon_2}\sinh\left(\frac{e\Psi_{particle}}{2k_BT}\right)\right) \tag{8}$$

Where, $\Psi_{particle}$ is the zeta potential of the orignal particle and e is the electron charge, k_B is the Boltzmann constant and T is the temperature. It must be noted that the image charge interaction can also be attractive. If the particle resides in a low dielectric medium, the image charge according to eqn 7 is opposite in sign, therefore image charge interactions are attractive. However, it is difficult to have particles in low dielectric medium in a charged state.

To model electrostatic double layer (EDL) interactions, a linear superposition approximation (LSA) method proposed in the literature was used as the interaction energies estimated with LSA are more realistic than the predictions of constant potential and constant charge models. The EDL interaction between the particle-interface and particle-image particle was calculated using eqn 9 and eqn 11, respectively.[46]

$$UE_{p-int} = UE_{p-int}(h) + UE_{p-int}(h+2r) + \frac{64\pi\varepsilon}{k}\left(\frac{k_BT}{ze}\right)^2\gamma_p\gamma_{int}[-e^{-kh} + e^{-k(h+2r)}] \tag{9}$$

$$UE_{p-int}(h) = 64\pi\varepsilon r\left(\frac{k_BT}{ze}\right)^2\gamma_p\gamma_{int}[-e^{-kh}] \tag{10}$$

$$UE_{p-image}(h) = 32\pi\varepsilon r\left(\frac{k_BT}{ze}\right)^2\gamma_p\gamma_{image}[-e^{-2kh}] \tag{11}$$

$$\gamma_p = \tanh\left(\frac{ze\Psi_p}{k_BT}\right) \tag{12}$$

$$\gamma_{int} = \tanh\left(\frac{ze\Psi_{int}}{k_BT}\right) \tag{13}$$

$$\gamma_{image} = \tanh\left(\frac{ze\Psi_{image}}{k_BT}\right) \tag{14}$$

Where, $\varepsilon = \varepsilon_0\varepsilon_r$, ε_0 is the dielectric permittivity of the vacuum, ε_r is the relative dielectric constant of water, r is the particle radius, h is the surface to surface distance, k^{-1} is the Debye length, Ψ is the surface potential, k_B is the Boltzmann constant, z is the valance of the ion, e is the electron charge and T is the temperature. In equations (9) to (14), the subscript p indicates particle, *int* indicates interface (in this case oil-water interface), *image* denotes image charge. The average particle size of 10 nm was used for the calculation of interaction potential. At low salt concentration (0.001 M), the individual contributions and the overall interaction energy as a function of separation distance is showed in Fig.5. From the Fig.5, the EDL interactions

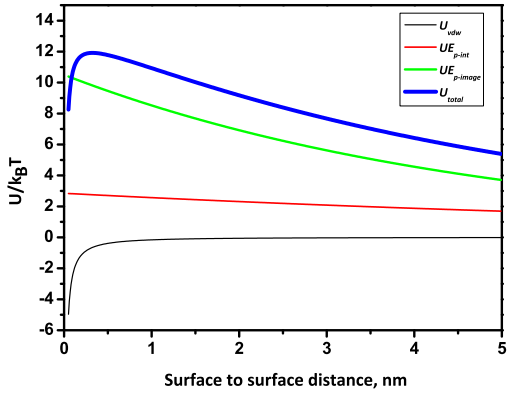

Fig. 5 The contribution of various interactions to the overall particle-interface interaction energy at 0.001 M NaCl concentration. The overall (U_{total}) energy barrier is more near the interface. At low salt concentration the image charge EDL interactions are dominating.

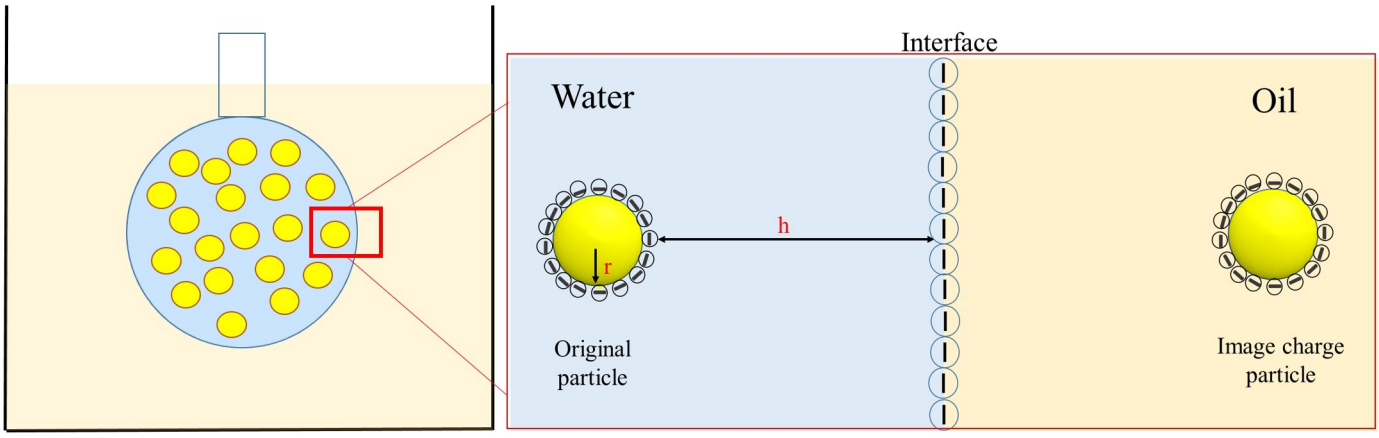

Fig. 4 Schematic diagram of a charged particle near to the interface and image charge. The particle of radius r at a distance h from the interface experiences repulsion from an image charge located at the same distance (h) in the oil phase.

between the particle-interface and particle-image charge are repulsive and van der Waals interaction is attractive. The overall interaction energy shows an energy barrier of $11.93k_BT$. The image charge repulsive energy is higher than the particle-interface repulsion energy and these interactions dominate at small surface to surface separation distance. So the thermal energy of the particle is not sufficient to overcome the energy barrier. Thus particles do not reach the interface and hence no adsorption. The overall interaction energy (U_{total}) at different salt concentration is calculated and shown in Fig 6. When the surface charge was screened by the addition of 0.05 M NaCl, the energy barrier reduces to $5.65k_BT$ (See Table 3). Correspondingly, a significant decrease in surface tension was observed when 0.05 M NaCl was added. However, at a higher salt concentration of 0.1 M NaCl, the overall interaction energy barrier is small and comparable to the thermal energy of the particles.

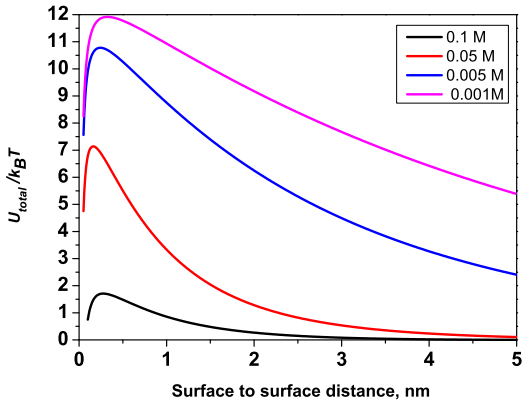

Fig. 6 The overall interaction (U_{total}) energy at different salt concentration as function of surface to surface distance.

Table 3 A comparison of the energy barrier calculated from early stage DST data and overall interactions. The effective diffusivity used in predicting energy barrier is also shown.

Salt concentration M	D_{eff} m^2/s	U/k_BT (from eq(5))	U_{total}/k_BT (DLVO+image)
0.001	$1.73\pm0.14\times10^{-15}$	10.27±0.07	11.93
0.005	$2.29\pm0.11\times10^{-15}$	9.98±0.05	10.74
0.05	$7.41\pm0.05\times10^{-15}$	8.81±0.01	5.65
0.1	$2.48\pm0.08\times10^{-14}$	7.61±0.04	1.70

The energy barrier calculated was $1.70\ k_BT$. Therefore, the particles were found to adsorb readily to the oil-water interface as confirmed by the DST measurements (see Fig. 2). The addition of salt decreases the zeta potential of the particles and as well as that of the oil-water interface (Table 2) resulting in reduced image charge and particle-interface repulsion. As the overall energy barrier is small, the thermal energy of the particles is sufficient to overcome this energy barrier. The energy barrier estimated from the DST data and the energy barrier calculated by considering the contribution of image charge repulsion to the overall interaction potential at different salt concentration are given Table 3. While the energy barriers do not match quantitatively, a similar trend can be seen. It was observed that the energy barrier from the two approaches monotonically decrease with increase in NaCl concentration as expected. The discrepancy is probably due to the fact that only pair wise interaction between particle and interface was used in overall interaction calculations. However, the DST measurements are a result of multi-particle interactions. The incorporation of multi-body interactions and size polydispersity in the overall interaction calculation would be more appropriate. At higher salt concentration the presence of aggregates that have

lower diffusivity may also contribute to this deviation.

3.4 Effect of particle concentration on adsorption kinetics

The kinetics of adsorption of particles to the interface depends on the particle diffusivity as well as on particle concentration. In the previous section we studied the effect of particle surface charge on adsorption process. To investigate the effect of particle concentration, we used a series of aqueous silica nanoparticle suspensions of concentrations ranging from 0.25, 0.5 and 1 wt % at two different fixed salt concentrations (0.1 and 0.05 M NaCl). The effect of particle concentration on the adsorption kinetics is shown in Fig.7. For 0.1 M NaCl concentration, as the particles concentration increases the change in the interfacial tension observed was more. Similar trends were observed at 0.05 M NaCl. With increase in particle concentration, the number particles in the drop increase and therefore, on an average there are more particles close to the oil-water interface. As the particles surface charge is screened due to the addition of NaCl, there is more adsorption of particles to the interface. Similar effect of particle concentration on adsorption kinetics has been reported.[20]

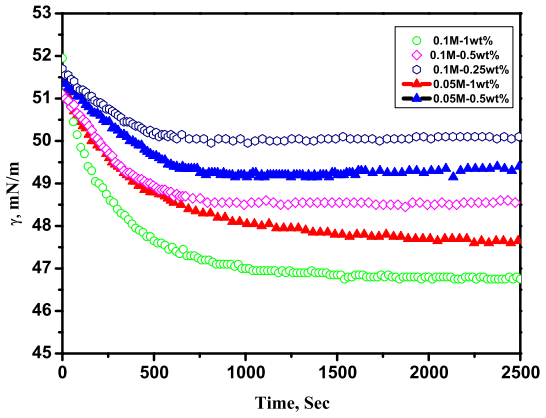

Fig. 7 The effect of particle concentration on the adsorption kinetics. The change in interfacial tension for two salt concentrations (0.1M and 0.05M) as varying the particle concentration (1, 0.5 and 0.25 wt%). The interfacial tension decrease is more at higher particle concentration.

3.5 Equilibrium coverage of particles at interface

From the pendant drop experiments and modeling of adsorption kinetics it is clear that the adsorption of particles at the interface strongly depends on salt concentration and initial concentration of particles in the bulk. A general feature of the time evolution of the surface tension is that a plateau in the surface tension is observed due to quasi-equilibrium coverage of the interface with adsorbed nanoparticles. When a pendant drop of aqueous silica dispersion is placed in oil medium for a sufficient long time ($t \to \infty$), the surface tension will reach a equilibrium value which indicates the maximum possible coverage of the particles at interface. From thermodynamics, this corresponds to the same chemical potential of particles in the bulk and at the interface. Therefore, the condition of equality of chemical potential can be used to calculate the equilibrium coverage of particles at the oil-water interface.[36,47]

The chemical potential of monodisperse spherical nanoparticles in the bulk is calculated by assuming the particles are equally charged. The particles are assumed to be present in the aqueous phase alone and the concentration is such that the interparticle interactions in the bulk are negligible. Under these conditions, the chemical potential of the charged nanoparticles in the bulk is given by[36]

$$\frac{\mu_{bulk}}{k_B T} = \log \frac{V_w}{V_p} + \log(\phi_b) + \frac{4\pi r^2 \gamma_{pw}}{k_B T} \tag{15}$$

In this equation, r is the particle radius, γ_{pw} is the interfacial tension between water (solvent) and the particle, V_p is the volume of the particle, V_w is the drop volume, and ϕ_b is the volume fraction of the particles in the bulk. In eqn (15) the first two terms take into account the entropic contribution and the last term is attributed to the surface free energy of the particle-water interface.

The chemical potential of a charged nanoparticles at the water-oil interface is due to contributions of (i) surface free energies of the water-oil, particle-water and particle-oil interfaces (ii) translational entropy of the particle at the interface (iii) interactions between the particles at interface. In this analysis, we consider the electrostatic interaction between the particles both dipole-dipole and coulomb interactions. However, the van der Waals interactions are neglected as their magnitude is very much small considered to long-range electrostatic interactions. Therefore, the overall chemical potential of the nanoparticles adsorbed at interface is

$$\frac{\mu_{int}}{k_B T} = \log \frac{A_i}{A_c} + \log(\phi_i) + \frac{A_{pw}\gamma_{pw} + A_{po}\gamma_{po} - A_c\gamma_{ow}}{k_B T} + \frac{E_{dd} + E_{coul}}{k_B T} \tag{16}$$

In this equation, A_i is the surface area of the drop, A_c is the cross sectional area of the particle at the interface, ϕ_i is the interface surface fraction, A_{pw} is the surface area of the particle in contact with water, A_{po} is the surface area of the particle in contact with oil, γ_{pw} is the particle-water interface tension, γ_{po} is the particle-oil interface tension, γ_{ow} is the oil-water interfacial tension, E_{dd} is the dipole-dipole interaction, and E_{coul} coulomb interaction.

At equilibrium the bulk and interface chemical potentials are equal. The electrostatic interactions are distance dependent and the coverage at interface is a function of distance between the particles. Therefore, the electrostatic interactions are calculated as a function of surface coverage and surface charge density of the particles. At equilibrium,

$$\log \frac{V_w}{V_p} + \log(\phi_b^{eq}) = \log \frac{A_i}{A_c} + \log(\phi_i^{eq}) + \frac{\Delta E + E_{dd} + E_{coul}}{k_B T} \tag{17}$$

where, $\Delta E = -(4\pi r^2 \gamma_{pw} - A_{pw}\gamma_{pw} - A_{po}\gamma_{po} + A_c\gamma_{ow})/(k_B T)$ is the energy of detachment of the particles from the interface also same as eqn 2. From eqn (17) the surface coverage at interface is

$$\frac{\phi_i^{eq} A_i}{A_c N_T} = \frac{1}{(1 + \exp\frac{(\Delta E + E_{dd} + E_{coul})}{k_B T})} \tag{18}$$

Where, N_T is the total number of particles in the droplet, E_{dd}

and E_{coul} are a function of surface coverage and surface charge density and ΔE depends on the three phase contact angle. The details of derivation of eqn18 is shown in the supporting information. We assume particles to be hexagonally arranged at interface and the net electrostatic interaction is the result of summation of interaction between the neighboring particles. The equilibrium surface coverage is calculated by solving the eqn (18) for a fixed charged density. As the actual charge density of the particle is not known and the calculation of charge density from the zeta potential will not give exact surface charge density, we have calculated the coverages as a function of salt concentration at different surface charge densities. The equilibrium surface coverage thus calculated are shown in fig (8). From Fig(8), as the particle charge density increases the surface coverage is found to decrease due to increase in dipole-dipole repulsion energy. From the graph, we can conclude that at fixed charge density the addition of salt will increase the coverage of the particle at interface. These results qualitatively support the observations of pendant drop experiments, that as the concentration of salt is increased, coverage of particle increases resulting in a decrease in interfacial tension.

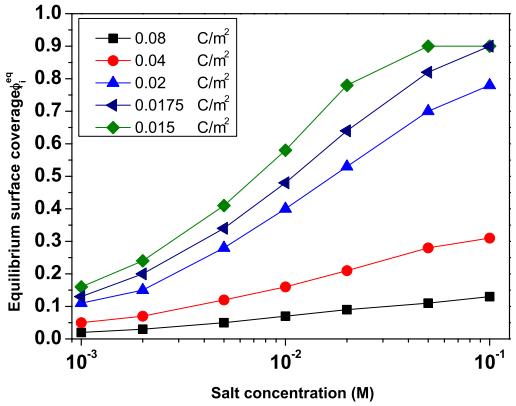

Fig. 8 Surface coverage as a function of salt concentration at different surface charge density. Surface coverage is increasing with increasing salt concentration due to reduction in the Debye length. Similarly decreasing in surface charge also promotes more coverage at interface.

4 Conclusion

In this work, we investigated the effect of particle charge and concentration on the adsorption dynamics of silica nanoparticles to the fluid-fluid interface. The experiments were conducted by considering a water drop containing monodispersed silica nanoparticle and decane as oil medium. The particle and interface charge was screened by the addition of NaCl. The adsorption of particles was monitored with a pendant drop tensiometer by recording the interfacial tension as a function of time. The interfacial tension decrease was more when the particles were weakly charged, i.e more number of particles were adsorbed to the interface. When the particles were highly charged, the interfacial tension change was negligible - that is - no adsorption of particles to the interface. We modeled the early stage DST data using the modified Ward and Tordai theory. From the model we calculated the effective diffusivity of the particles at different salt concentration. We show that the change in the effective diffusivity is due to the energy barrier as the particles approach near the interface. The energy barrier estimated from DST data corroborates well with the energy barrier calculated from the overall interactions taking into account the image charge effect. When the particles are highly charged, a high net energy barrier prevents the adsorption of particles to the interface. When the particle surface charge was screened with the addition of sufficient amount of NaCl, the net energy barrier decreases considerably and hence the particles readily adsorb to the oil-water interface. With increase in particle concentration, there was pronounced reduction in interfacial tension suggesting an increase in the population of particles at the oil-water interface. We conclude that the image charge interactions play an important role in adsorption of particles to interface and these studies will have implications on the use of particles for stabilization of incompatible interfaces. We have observed a similar effect of particle surface charge on the adsorption behavior of shape anisotropic particles.[48] An analytical expression that qualitatively captures the effect of surface charge on the equilibrium surface coverage of particles at the drop surface is derived by equating the chemical potential of the nanoparticles in the bulk with those adsorbed at the oil-water interface.

References

1 B. Binks and S. Lumsdon, *Langmuir*, 2001, **17**, 4540–4547.
2 B. Madivala, S. Vandebril, J. Fransaer and J. Vermant, *Soft Matter*, 2009, **5**, 1717–1727.
3 A. B. Pawar, M. Caggioni, R. Ergun, R. W. Hartel and P. T. Spicer, *Soft Matter*, 2011, **7**, 7710–7716.
4 J. Wang, F. Yang, J. Tan, G. Liu, J. Xu and D. Sun, *Langmuir*, 2009, **26**, 5397–5404.
5 H. Wang, V. Singh and S. H. Behrens, *The Journal of Physical Chemistry Letters*, 2012, **3**, 2986–2990.
6 A. Stocco, E. Rio, B. P. Binks and D. Langevin, *Soft Matter*, 2011, **7**, 1260–1267.
7 B. P. Binks and T. S. Horozov, *Angewandte Chemie*, 2005, **117**, 3788–3791.
8 B. P. Binks, R. Murakami, S. P. Armes, S. Fujii and A. Schmid, *Langmuir*, 2007, **23**, 8691–8694.
9 S. Fujii, P. Iddon, A. Ryan and S. Armes, *Langmuir*, 2006, **22**, 7512–7520.
10 J. W. Tavacoli, J. H. J. Thijssen, A. B. Schofield and P. S. Clegg, *Advanced Functional Materials*, 2011, **21**, 2020–2027.
11 M. N. Lee, J. H. Thijssen, J. A. Witt, P. S. Clegg and A. Mohraz, *Advanced Functional Materials*, 2013, **23**, 417–423.
12 J. W. Tavacoli, J. H. Thijssen, A. B. Schofield and P. S. Clegg, *Advanced Functional Materials*, 2011, **21**, 2020–2027.
13 T. Nallamilli, B. P. Binks, E. Mani and M. G. Basavaraj, *Langmuir*, 2015, **31**, 11200–11208.
14 S. D. C. Pushpam, M. G. Basavaraj and E. Mani, *Physical Review E*, 2015, **92**, 052314.
15 R. Aveyard, J. H. Clint, D. Nees and V. N. Paunov, *Langmuir*, 2000, **16**, 1969–1979.

16 W. Chen, S. Tan, T.-K. Ng, W. T. Ford and P. Tong, *Physical review letters*, 2005, **95**, 218301.
17 B. Madivala, J. Fransaer and J. Vermant, *Langmuir*, 2009, **25**, 2718–2728.
18 A. Würger, *EPL (Europhysics Letters)*, 2006, **75**, 978.
19 T. S. Horozov, R. Aveyard, J. H. Clint and B. P. Binks, *Langmuir*, 2003, **19**, 2822–2829.
20 N. Bizmark, M. A. Ioannidis and D. E. Henneke, *Langmuir*, 2014, **30**, 710–717.
21 O. S. Deshmukh, D. van den Ende, M. C. Stuart, F. Mugele and M. H. Duits, *Advances in colloid and interface science*, 2014.
22 K. Du, E. Glogowski, T. Emrick, T. P. Russell and A. D. Dinsmore, *Langmuir*, 2010, **26**, 12518–12522.
23 S. Ferdous, M. A. Ioannidis and D. Henneke, *Journal of Nanoparticle Research*, 2011, **13**, 6579–6589.
24 V. Garbin, J. C. Crocker and K. J. Stebe, *Langmuir*, 2011, **28**, 1663–1667.
25 N. Glaser, D. J. Adams, A. Böker and G. Krausch, *Langmuir*, 2006, **22**, 5227–5229.
26 A. Nelson, D. Wang, K. Koynov and L. Isa, *Soft matter*, 2015, **11**, 118–129.
27 Z. Sun, T. Feng and T. P. Russell, *Langmuir*, 2013, **29**, 13407–13413.
28 S. Kutuzov, J. He, R. Tangirala, T. Emrick, T. Russell and A. Böker, *Physical Chemistry Chemical Physics*, 2007, **9**, 6351–6358.
29 S. Rana, X. Yu, D. Patra, D. F. Moyano, O. R. Miranda, I. Hussain and V. M. Rotello, *Langmuir*, 2011, **28**, 2023–2027.
30 A. Ward and L. Tordai, *The Journal of Chemical Physics*, 1946, **14**, 453–461.
31 T. D. Gurkov, *Colloid and Polymer Science*, 2011, **289**, 1905–1915.
32 F. Ravera, L. Liggieri and A. Steinchen, *Journal of Colloid and Interface Science*, 1993, **156**, 109 – 116.
33 L. Liggieri, F. Ravera and A. Passerone, *Colloids and surfaces A: physicochemical and engineering aspects*, 1996, **114**, 351–359.
34 S. N. Moorkanikkara and D. Blankschtein, *Journal of colloid and interface science*, 2006, **296**, 442–457.
35 P. C. Hiemenz and R. Rajagopalan, *Principles of Colloid and Surface Chemistry, revised and expanded*, CRC press, 1997, vol. 14.
36 F. Reincke, W. K. Kegel, H. Zhang, M. Nolte, D. Wang, D. Vanmaekelbergh and H. Möhwald, *Physical Chemistry Chemical Physics*, 2006, **8**, 3828–3835.
37 P. A. Wierenga, M. B. Meinders, M. R. Egmond, F. A. Voragen and H. H. de Jongh, *Langmuir*, 2003, **19**, 8964–8970.
38 K. B. Song and S. Damodaran, *Langmuir*, 1991, **7**, 2737–2742.
39 S. G. Kluijtmans, E. H. de Hoog and A. P. Philipse, *The Journal of chemical physics*, 1998, **108**, 7469–7477.
40 B. P. Binks, L. Isa and A. T. Tyowua, *Langmuir*, 2013, **29**, 4923–4927.
41 R. Aveyard, B. P. Binks and J. H. Clint, *Advances in Colloid and Interface Science*, 2003, **100**, 503–546.
42 K. Marinova, R. Alargova, N. Denkov, O. Velev, D. Petsev, I. Ivanov and R. Borwankar, *Langmuir*, 1996, **12**, 2045–2051.
43 S. Bhattacharjee and M. Elimelech, *Journal of colloid and interface science*, 1997, **193**, 273–285.
44 L. Bergström, *Advances in Colloid and Interface Science*, 1997, **70**, 125–169.
45 J. N. Israelachvili, *Intermolecular and surface forces: revised third edition*, Academic press, 2011.
46 S. Lin and M. R. Wiesner, *Langmuir*, 2010, **26**, 16638–16641.
47 V. N. Paunov, B. P. Binks and N. P. Ashby, *Langmuir*, 2002, **18**, 6946–6955.
48 V. R. Dugyala, T. G. Anjali, S. Upendar, E. Mani and M. G. Basavaraj, *Farady discussion*, 2015, doi:10.1039/C5FD00136F.